

RSC Advances



This is an *Accepted Manuscript*, which has been through the Royal Society of Chemistry peer review process and has been accepted for publication.

Accepted Manuscripts are published online shortly after acceptance, before technical editing, formatting and proof reading. Using this free service, authors can make their results available to the community, in citable form, before we publish the edited article. This *Accepted Manuscript* will be replaced by the edited, formatted and paginated article as soon as this is available.

You can find more information about *Accepted Manuscripts* in the [Information for Authors](#).

Please note that technical editing may introduce minor changes to the text and/or graphics, which may alter content. The journal's standard [Terms & Conditions](#) and the [Ethical guidelines](#) still apply. In no event shall the Royal Society of Chemistry be held responsible for any errors or omissions in this *Accepted Manuscript* or any consequences arising from the use of any information it contains.

Supramolecular Functionalized Polybenzoxazines from Azobenzene Carboxylic Acid/Azobenzene Pyridine Complexes: Synthesis, Surface Properties, and Specific Interactions

Mohamed Gamal Mohamed,^a Chi-Hui Hsiao^a, Kuo-Chih Hsu^a, Fang-Hsien Lu,^b His-Kang Shih,^b and Shiao-Wei Kuo^{a,*}

Received (in XXX, XXX) Xth XXXXXXXXX 200X, Accepted Xth XXXXXXXXX 200X

DOI: 10.1039/b000000x

In this study we synthesized Azo-COOH BZ, a new benzoxazine derivative containing both azobenzene and carboxylic acid units, through the reaction of 4-(4-hydroxyphenylazo)benzoic acid (Azo-COOH, itself prepared through a diazonium reaction of 4-aminobenzoic acid with phenol in the presence sodium nitrite and NaOH) with paraformaldehyde and aniline in 1,4-dioxane. Fourier transform infrared (FTIR) spectroscopy and ¹H and ¹³C nuclear magnetic resonance spectroscopy confirmed the chemical structure of Azo-COOH BZ. We used differential scanning calorimetry (DSC), thermogravimetric analysis, and FTIR spectroscopy to investigate the curing behavior of this new benzoxazine monomer. DSC revealed that the exothermic peak representing the ring opening polymerization of the benzoxazine unit appeared at low temperature relative to those of typical benzoxazines, indicating that the presence of the carboxylic acid and azobenzene units of this monomer catalyzing the benzoxazine ring opening reaction. In addition, blending with various molar ratios of a benzoxazine monomer presenting a pyridyl unit (Azopy BZ) led to strong intermolecular hydrogen bonding between the CO₂H group of Azo-COOH BZ and the pyridyl group of Azopy BZ. These supramolecular complex systems also featured significantly lower curing temperatures (down from ca. 200 °C of Azo-COOH BZ to 150 °C of supramolecular complex), with their products retaining the high water contact angles required for low-surface-energy applications.

Introduction

Heterocyclic benzoxazine monomers can be synthesized through Mannich condensations of phenols, aldehydes, and amines in the absence of initiators; subsequent thermal activation can lead to polymerization of the monomers.¹ The diversity of applicable phenols and amines offers remarkable flexibility in the molecular design of suitable benzoxazine monomers. Polybenzoxazines (PBZs) are easy-to-process phenolic resins that possess excellent thermal and mechanical properties, low water absorption, high contents of carbon residues, low surface energies, good flame-retardancy, and near-zero volumetric shrinkage/expansion upon polymerization.²⁻¹⁴ Furthermore, PBZs have superb molecular design flexibility and can be synthesized through ring opening polymerizations of aromatic benzoxazines with no need for strong catalysts and without the production of polymerization byproducts.¹⁵⁻¹⁸

For specific applications, the thermal and mechanical properties of PBZs can be modified in many ways. For example, benzoxazine monomers presenting allyl,¹⁹ acetylene,²⁰ propargyl,²¹ nitrile,²² and maleimide²³ functionalities have been prepared to facilitate additional cross-linking upon thermal curing. The thermal and mechanical properties of PBZs can also be improved through the formation of blends, copolymers, and inorganic nanocomposites.²⁴⁻³² Another interesting use of functionalized benzoxazine monomers is their combination with inorganic materials to fabricate nanocomposites, exploiting the attractive interactions between the polar functional groups of the monomers and the inorganic surfaces. For example, Yagci et al.

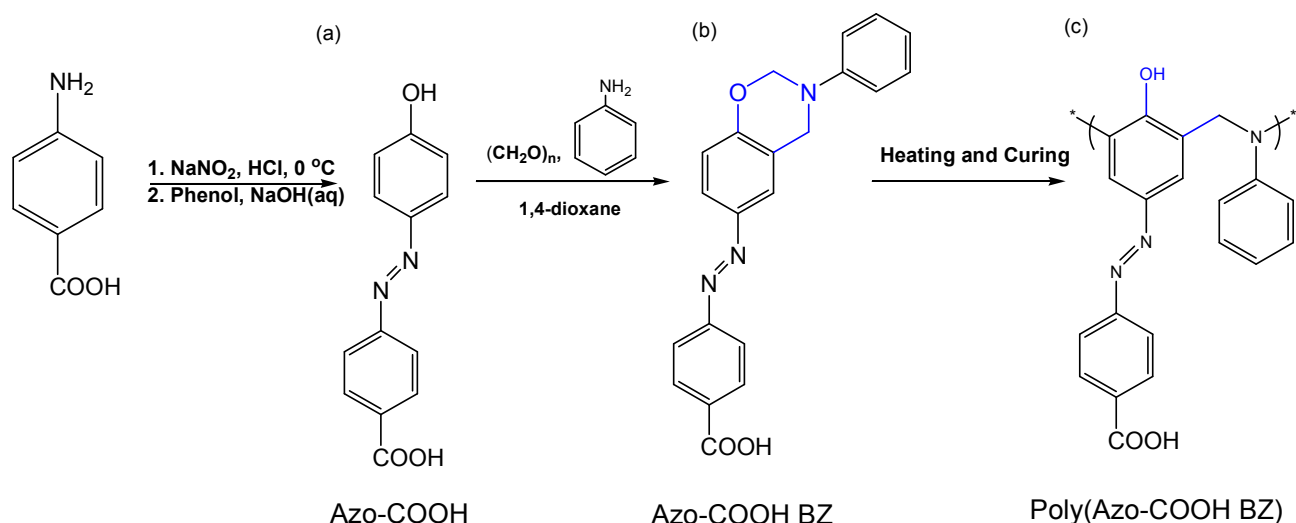
reported the attachment of benzoxazine monomers bearing carboxyl groups onto the surface of magnetite nanoparticles;³³ they also developed a PBZ/montmorillonite nanocomposite, using a benzoxazine bearing a 4-pyridyl moiety as a key material.³³

Azopyridine benzoxazine derivatives have the attractive features of being light-active, because of their azobenzene units, and having the ability of self-assemble through hydrogen bonding of their pyridyl units with organic acids.³³ Endo et al. reported a novel benzoxazine bearing a 4-aminopyridyl moiety, synthesized from 4-aminopyridine, *p*-cresol, and paraformaldehyde, with addition of acetic acid being necessary to neutralize the basicity of the system; the presence of 4-aminopyridyl moieties imparted the resulting polymer with high affinity toward metal ions [e.g., copper(II) and cobalt(II)], leading to the formation of the corresponding polymer-metal complexes, and the formation of insoluble colored precipitates.³⁴ Although benzoxazine derivatives can be cured at elevated temperatures without the need for catalysts, the addition of weak or strong acids can lower the curing temperature.³⁵ Recently, Andreu et al. reported that the presence of carboxyl groups in the structure of a benzoxazine monomer impacted the thermal curing process and lowered the processing temperatures.³⁶

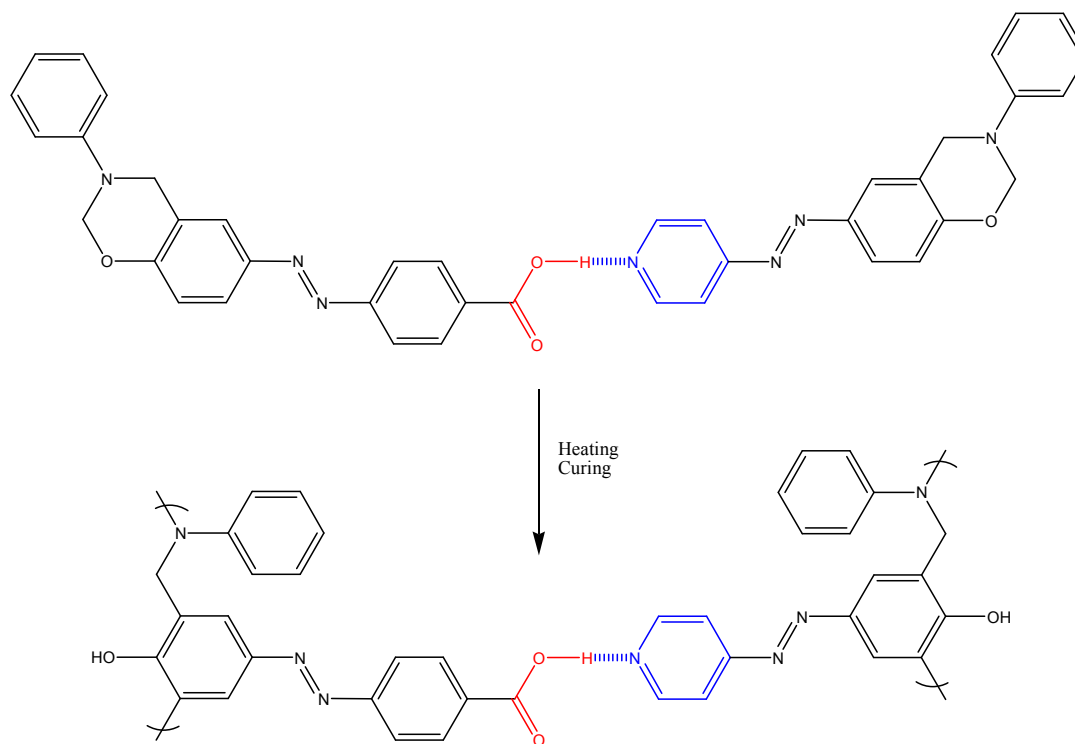
Stimuli-responsive materials are receiving a great deal of attention at present. Various stimuli (e.g., pH; ionic strength; solvent vapor; light; heat; electrical field) can be used to affect the properties and conformations of polymers.³⁷⁻³⁹ Polymers containing azobenzene moieties are of particular interest because of the reversibility of their photo-isomerizations and of their thermal cis-to-trans isomerizations.^{40,41} Interconversions between ground state trans forms and higher-energy cis forms can be achieved both photochemically (trans-to-cis) and thermally (cis-to-trans) with high degrees of efficiency and the absence of competing side reactions. Because one configurational isomer is furnished photochemically while the other is favored thermally, it is possible to effectively switch azobenzene-modified species into desired geometries and polarities. Thus, the incorporation of azobenzene moieties into PBZs might impart them with photo-

^aDepartment of Materials and Optoelectronic Science, Center for Functional Polymers and Supramolecular Materials, National Sun Yat-Sen University, Kaohsiung, Taiwan
E-mail: kuosw@faculty.nsysu.edu.tw

^bInstitute of Applied Chemistry, National Chiao-Tung University, Hsinchu, Taiwan



Scheme 1. Synthesis of Azo-COOH, Azo-COOH BZ, and poly(Azo-COOH BZ).



Scheme 2. Hydrogen bonding between Azo-COOH BZ and Azopy BZ monomers and in their corresponding polymer blends.

and thermo-regulated behavior when subjected to changes in incident light or heat.^{42–44}

PBZs are also interesting materials because of their strong intramolecular hydrogen bonding after curing and their extremely low surface energies—in some cases lower than that of pure Teflon.⁴⁵ Nevertheless, the need for high curing temperatures limits the applications of PBZs, especially for use as polymer coatings. Recently, a method for lowering the curing temperature of PBZs attracted great interest because it broadened the applicability of PBZs in temperature-sensitive substrates (e.g., most polymeric materials). Chang et al. reported that bis(3-allyl-

3,4-dihydro-2H-1,3-benzoxazinyl)isopropane (B-ala) can be cured at a low temperature ($120\text{ }^\circ\text{C}$) with the aid of 2,2'-azobisobutyronitrile (AIBN), resulting in a PBZ displaying record-low surface energy.⁴⁶ Most polymer coatings possessing photoresponsive wettability behavior are based on rough surfaces modified to become more hydrophilic or hydrophobic upon exposure to light. Jiang et al. reported that covalent attachment of azobenzene-functionalized polyacrylamides to a rough surface led to large contact angles after photoisomerization.⁴⁷

In this study, we synthesized a new benzoxazine derivative, Azo-COOH BZ, containing both azobenzene and carboxylic acid

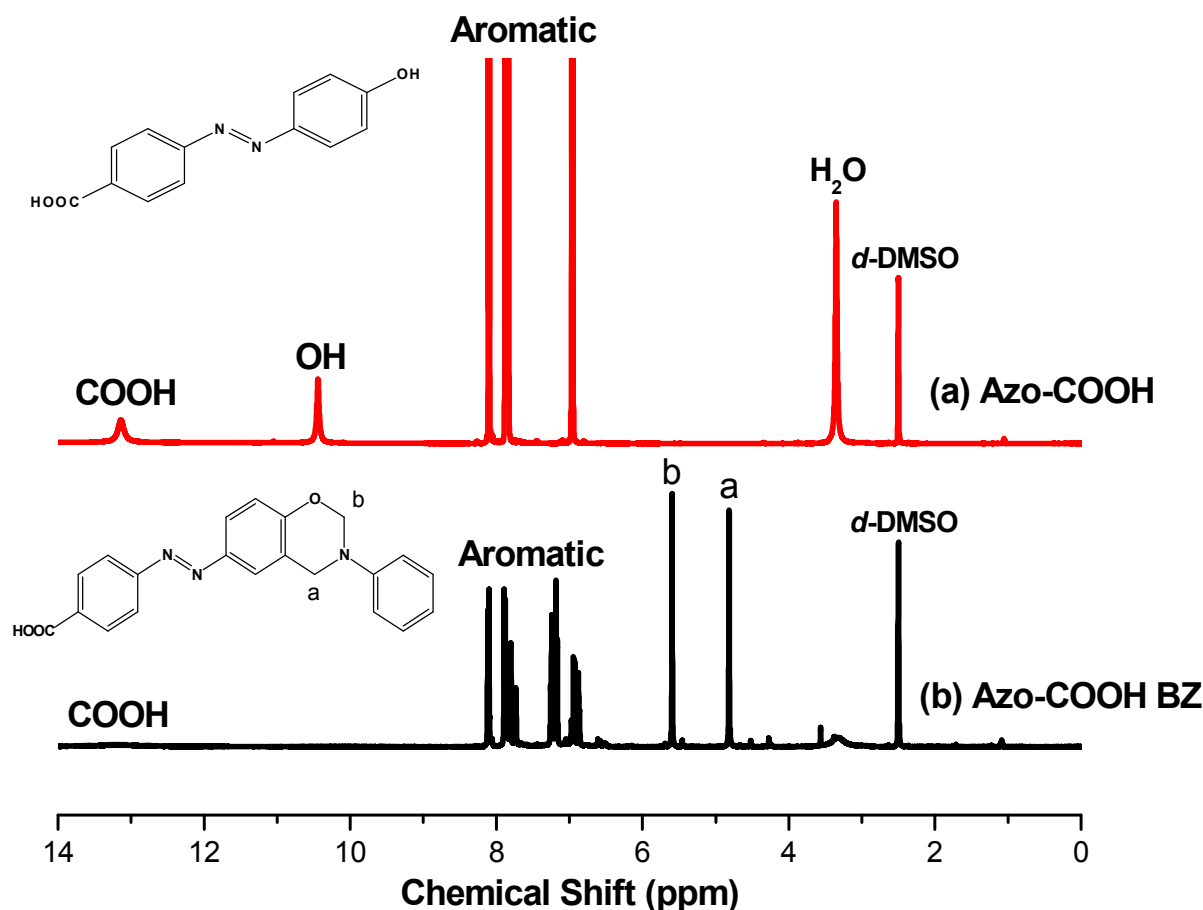


Figure 1. ^1H NMR spectra of (a) Azo-COOH and (b) Azo-COOH BZ.

moieties. First, we prepared 4-(4-hydroxyphenylazo)benzoic acid (Azo-COOH) through a diazonium reaction of 4-aminobenzoic acid with phenol in the presence of NaOH [Scheme 1(a)]. We then formed Azo-COOH BZ through the reaction of Azo-COOH, paraformaldehyde, and aniline in 1,4-dioxane [Scheme 1(b)]. Subsequently, we examined, before and after curing, the physical properties of Azo-COOH BZ when blended at various molar ratios with a benzoxazine monomer possessing a pyridyl unit (Azopy BZ) that can form intermolecular hydrogen bonds [Scheme 2]. We used differential scanning calorimetry (DSC), Fourier transform infrared (FTIR) spectroscopy, and contact angle analyses to examine the thermal properties, specific interactions, and surface behavior of these supramolecular PBZ materials.

Experimental Section

Materials

4-Aminobenzoic acid, paraformaldehyde (96%), sodium nitrite (99%), hydrochloric acid (ca. 37%), aniline (99.8%), EtOAc, EtOH, and hexane were purchased from Acros and used as received. 1,4-Dioxane and NaOH were purchased from Aldrich. Azopy-BZ was synthesized using a previously reported procedure.⁴⁸

4-(4-Hydroxyphenylazo)benzoic Acid (Azo-COOH)

A solution of 4-aminobenzoic acid (13.7 g, 0.100 mol) in dilute HCl [a mixture of conc. HCl (20 mL) in water (20 mL)] was diazotized by the addition of a solution of sodium nitrite (6.90 g,

0.100 mol) in water (20 mL). The mixture was stirred at 0 °C and then diluted with cooled MeOH (400 mL). Phenol (9.41 g, 0.100 mol), dissolved in a chilled solution of NaOH (10.8 g, 0.190 mol) in MeOH (100 mL), was added dropwise to the solution containing the diazonium salt. A red dye formed; this mixture was stirred for 2 h and then poured into dilute HCl with stirring. The red solid was filtered off, washed thoroughly with water, dried, and purified through column chromatography (SiO_2 ; *n*-hexane/EtOAc, 1:1). Recrystallization (MeOH/ H_2O) gave the product (9.5 g, 76%). M.p.: 273–275 °C (DSC). ^1H NMR (δ , d_6 -DMSO): 6.88–8.12 (m, 8H), 10.17 (s, OH), 13.13 (s, COOH). ^{13}C NMR (δ , d_6 -DMSO): 167.20 (C=O), 162.28, 154.70, 145.52, 132.35, 130.37, 126.12, 121.83, 116.57. IR (KBr, cm^{-1}): 3204–3463 (OH), 3053–2500 (COOH), 1660 (C=O).

(*E*)-4-((3-Phenyl-3,4-dihydro-2H-benzo[*e*] [1, 3] benzoic Acid (Azo-COOH BZ)

A solution of aniline (0.420 g, 4.54 mmol) in 1,4-dioxane (25 mL) was added portionwise to a stirred solution of paraformaldehyde (0.270 g, 8.67 mmol) in 1,4-dioxane (100 mL) in a 250-mL flask, cooled in an ice bath. The mixture was then stirred for 20 min while maintaining the temperature below 5 °C and then a solution of 4-(4-hydroxyphenylazo)benzoic acid (1.00 g, 4.13 mmol) in 1,4-dioxane (30 mL) was added. The mixture was heated under reflux at 110 °C for 24 h. After cooling, the solvent was removed in a rotary evaporator; the viscous residue was dissolved in EtOAc (100 mL) and washed several times with 5% NaHCO_3 and

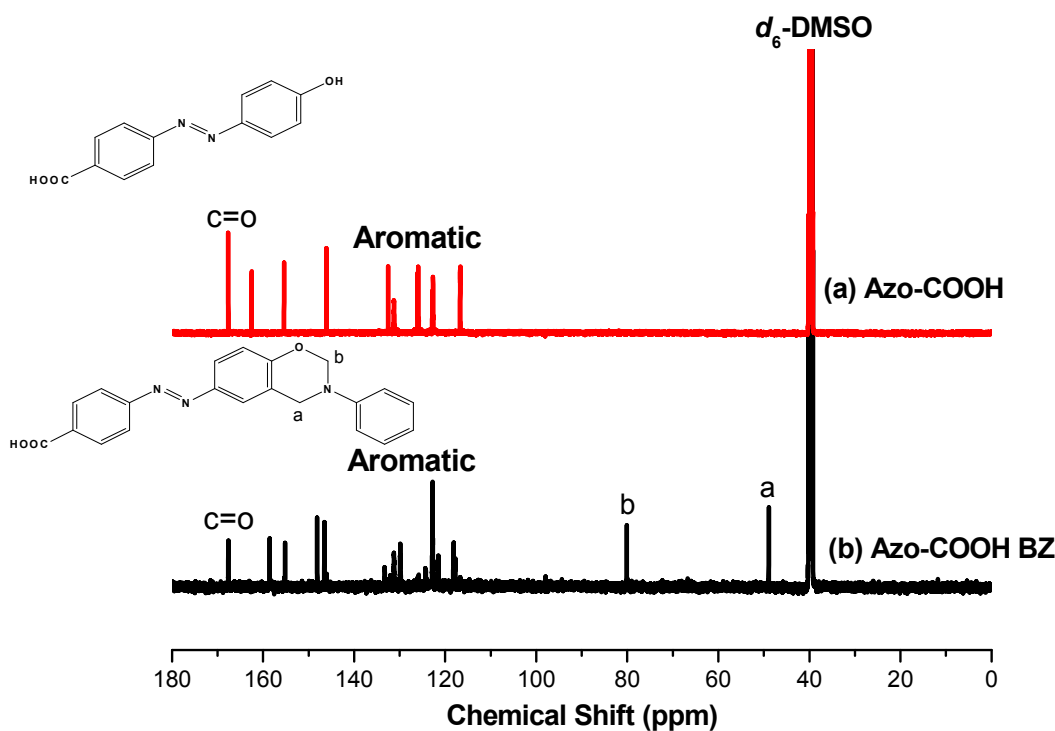


Figure 2. ^{13}C NMR spectra of (a) Azo-COOH and (b) Azo-COOH BZ.

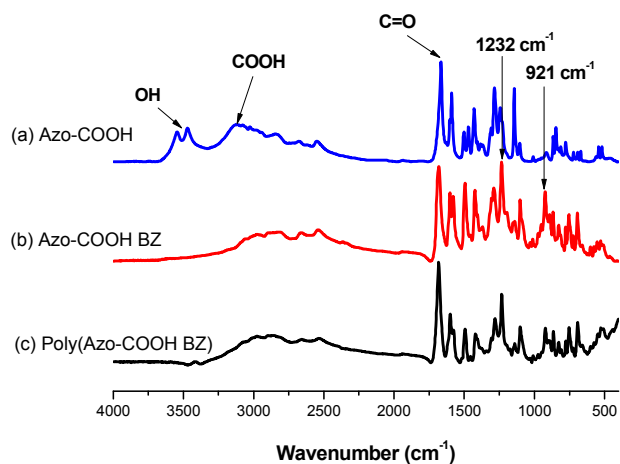


Figure 3. FTIR spectra of (a) Azo-COOH, (b) Azo-COOH BZ, and (c) poly(Azo-COOH BZ), recorded at room temperature.

finally with distilled water. The organic phase was dried (MgSO_4) and concentrated under vacuum to afford an orange residue, which was purified through column chromatography (SiO_2 ; *n*-hexane/EtOAc, 1:1) to give an orange powder (1.1 g, 70%). ^1H NMR (δ , d_6 -DMSO): 4.84 (s, 2H, CH_2N), 5.59 (s, 2H, OCH_2N), 6.94 (s, 2H, CH), 6.94 (s, 2H), 7.01 (d, 2H), 7.23 (d, 2H), 7.76 (d, 2H), 8.09 (d, 2H), 8.12 (d, 2H). ^{13}C NMR (δ , d_6 -DMSO): 48.47 (CCH_2N), 80.04 (OCH_2N), 117.54–158.02 (aromatic), 167.2 ($\text{C}=\text{O}$). IR (KBr, cm^{-1}): 1232 (asymmetric C–O–C stretching), 1341 (CH_2 wagging), 921 and 1490 (trisubstituted benzene ring stretching), 1441 (stretching of trans $\text{N}=\text{N}$ bond), 3053–2500 (COOH), 1660 ($\text{C}=\text{O}$).

Azo-COOH BZ/Azopy BZ Complexes

Azo-COOH BZ and Azopy-BZ, at a chosen molar ratio, were dissolved in THF to obtain a homogeneous solution. After most

of the solvent had evaporated slowly at room temperature under atmosphere pressure, the mixture was dried in a vacuum oven at 30°C for approximately 20 h.

Characterization

^1H and ^{13}C nuclear magnetic resonance (NMR) spectra were recorded using an INOVA 500 instrument, with DMSO as the solvent and TMS as the external standard. FTIR spectra of the polymer films were recorded using a Bruker Tensor 27 FTIR spectrophotometer and the conventional KBr disk method; 32 scans were collected at a spectral resolution of 4 cm^{-1} . The prepared films were sufficiently thin to obey the Beer–Lambert law. FTIR spectra recorded at elevated temperatures were obtained using a cell mounted within the temperature-controlled compartment of the spectrometer. The thermal stability of the samples was measured using a TG Q-50 thermogravimetric analyzer operated under a N_2 atmosphere. The cured sample (ca. 5 mg) was placed in a Pt cell and heated at a rate of $20^\circ\text{C min}^{-1}$ from 30 to 800°C under a N_2 flow rate of 60 mL min^{-1} . The UV–Vis spectrum of Azo-COOH BZ (10^{-4} M in THF) was recorded using a Shimadzu mini 1240 spectrophotometer. The photoisomerizations of Azo-COOH BZ were performed by using a UV–Vis lamp in conjunction with 365-nm (90 mW cm^{-2}) and $400\text{–}500\text{-nm}$ (90 mW cm^{-2}) filters to generate the UV or visible light for the respective trans-to-cis and cis-to-trans isomerizations. The contact angles of $5\text{-}\mu\text{L}$ drops of deionized water on the polymer samples before and after curing were measured at 25°C using an FDSA Magic Droplet 100 contact angle goniometer interfaced with image capture software. We measured contact angles on the surface of a film by dissolving an appropriate concentration of Azo-COOH BZ (trans form) in THF, then drop this solution on glass as substrate then curing at various temperature by spin coating. For measuring contact angle of cis form, we exposed the trans form solution to UV lamp at 365 nm to change the isomer then drop this solution on substrate and curing at various temperature.

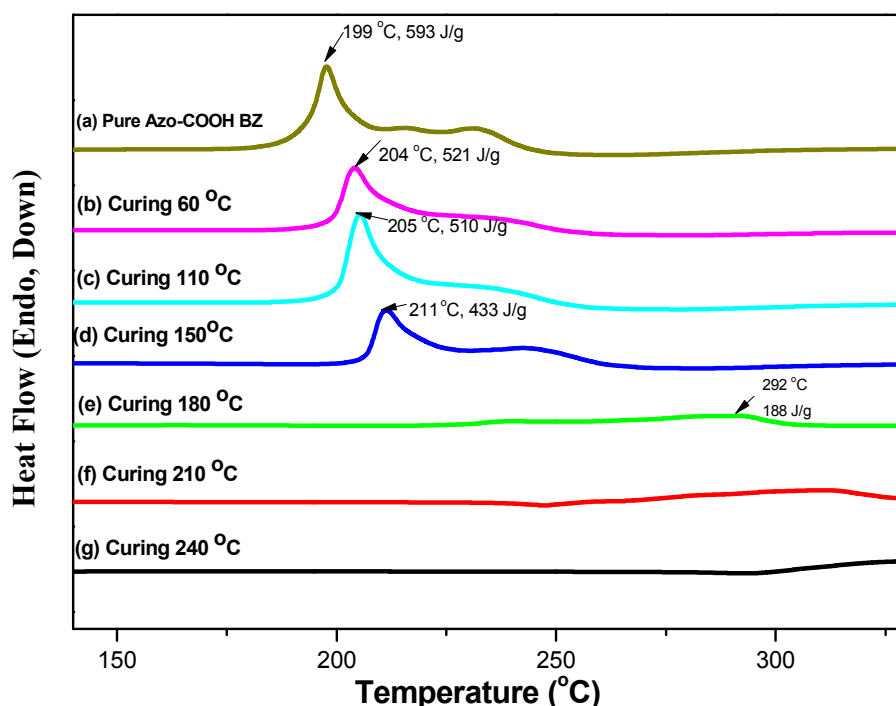


Figure 4. DSC thermograms of the Azo-COOH BZ monomer, recorded after each heating stage (2 h at each temperature).

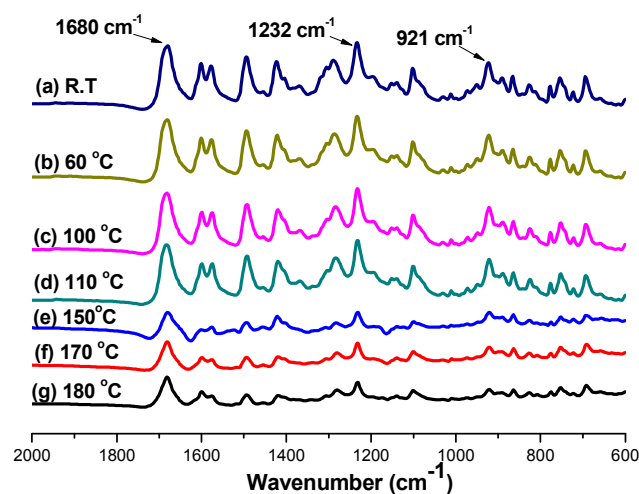


Figure 5. FTIR spectra of the Azo-COOH BZ monomer, recorded after each heating stage.

10 Results and Discussion

Synthesis of Azo-COOH BZ through Mannich Reaction of Azo-COOH with Aniline and Paraformaldehyde

We prepared Azo-COOH BZ in high purity and high yield through a Mannich reaction of Azo-COOH, phenol, and aniline in 1,4-dioxane at 110 °C (Scheme 1). Figure 1 presents the ¹H NMR spectra of Azo-COOH and Azo-COOH BZ. The spectrum of Azo-COOH [Figure 1(a)] features signals at 10.47 and 13.13 ppm representing the OH groups of the phenolic and COOH units, respectively. The aromatic protons of Azo-COOH appeared as signals in the range 6.97–8.10 ppm. The spectrum of Azo-COOH BZ [Figure 1(b)] features two characteristic peaks at 4.82 and 5.64 ppm, corresponding to the CH₂N and OCH₂N units, respectively, of the oxazine moiety. The signal for the OH group

of the phenolic moiety of Azo-COOH was absent in the spectrum of Azo-COOH BZ, but the aromatic signals of Azo-COOH remained, confirming the successful synthesis of Azo-COOH BZ.

Figure 2 presents the ¹³C NMR spectra of Azo-COOH and Azo-COOH BZ. In the spectrum of Azo-COOH, the signals of the azobenzene moiety appear in the range 116.57–162.28 ppm, with a signal at 167.20 ppm corresponding to the C=O group. In the spectrum of Azo-COOH BZ, two characteristic peaks appear at 48.47 and 80.04 ppm, representing the carbon nuclei of the oxazine moiety; signals for the azobenzene moiety are also evident, confirming the successful synthesis of Azo-COOH BZ.

Figure 3 presents the room-temperature FTIR spectra of Azo-COOH and Azo-COOH BZ and, after thermal curing, poly(Azo-COOH BZ). The spectrum of Azo-COOH features a sharp signal for the OH group at 3470 cm⁻¹, a broad signal at 3053–2523 cm⁻¹ for the intramolecularly hydrogen bonded CO₂H group, and absorption bands of the aromatic ring at 3025, 1610, and 1571 cm⁻¹. In the spectrum of Azo-COOH BZ, the signal for the OH group of the phenol unit is absent, but signals are evident for the C–C stretching vibrations of the 1,2,4-trisubstituted benzene ring (1490 and 921 cm⁻¹), for asymmetric C–O–C stretching (1232 cm⁻¹), and for stretching of the trans N=N unit (1440 cm⁻¹).

Together, these NMR and FTIR spectroscopic data confirmed the successful synthesis of Azo-COOH BZ. The FTIR spectrum recorded after thermal curing of pure Azo-COOH BZ at 180 °C features less-intense characteristic absorption bands for the trisubstituted aromatic ring of Azo-COOH BZ (1490 and 921 cm⁻¹) was decreased. The broad absorption bands in the range 2600–3500 cm⁻¹ in Figure 3(c) represent several different kinds of hydrogen bonding interactions: [O⁻⋯H–N⁺] and [COOH dimer] intramolecular hydrogen bonding near 2800 cm⁻¹, [O–H⋯N] intramolecular hydrogen bonding near 3200 cm⁻¹, and [O–H⋯O] intermolecular hydrogen bonding near 3342 cm⁻¹; the identities of these signals have been confirmed previously.⁴⁹

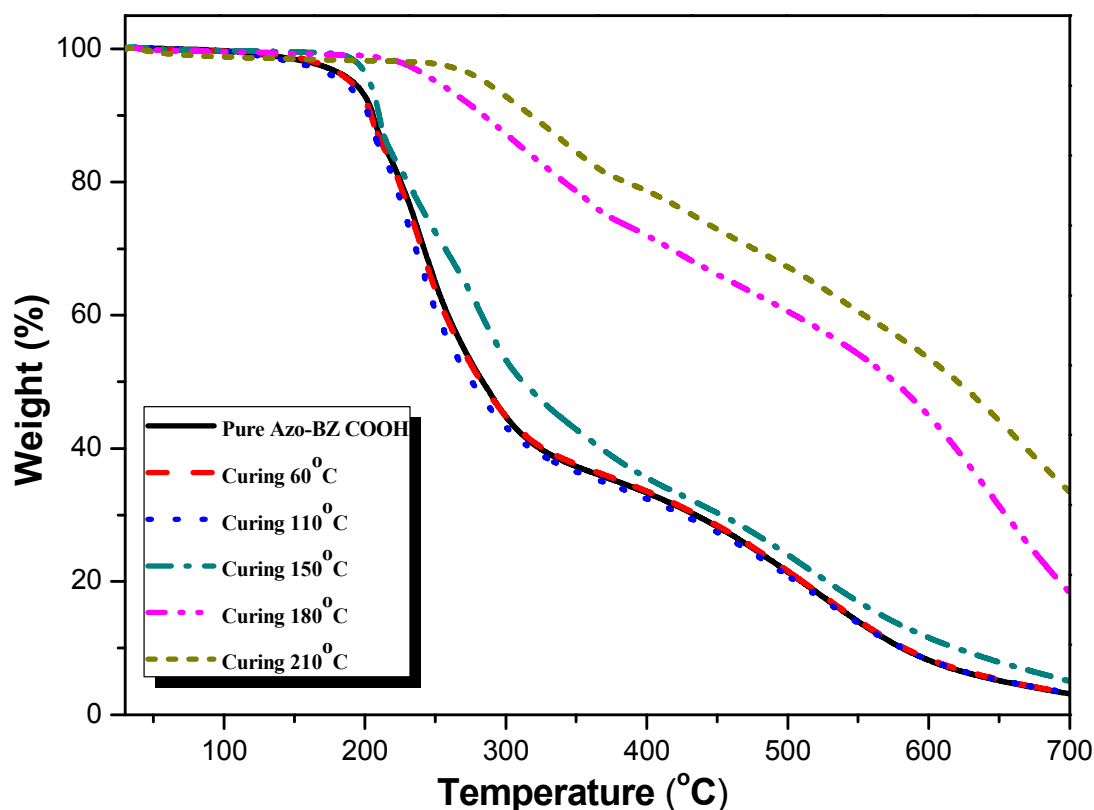


Figure 6. TGA analyses of Azopy-BZ, recorded after each curing stage

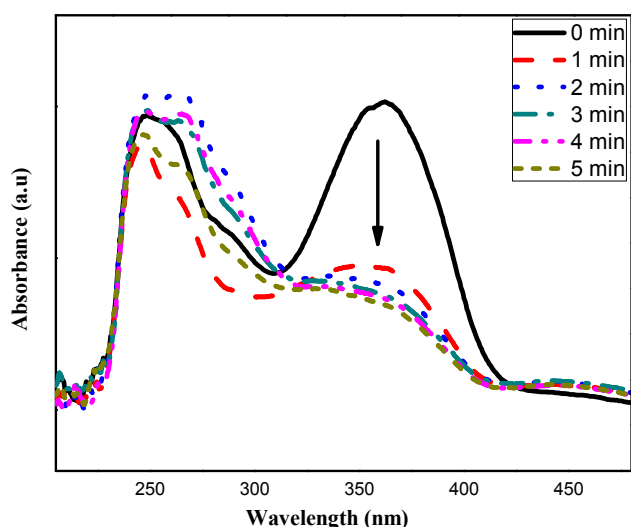


Figure 7. UV-Vis absorption spectra of Azo-COOH (10^{-4} M in THF) after treatment under UV light at 365 nm for various periods of time.

Thermal Polymerization of Azo-COOH BZ

We used DSC to determine the curing behavior of pure Azo-COOH BZ (Figure 4). The DSC trace of uncured Azo-COOH BZ features a sharp exothermic peak, attributed to its ring-opening polymerization, with the onset at 190 °C, the maximum at 199 °C, and a reaction heat of 593 J g⁻¹. The curing temperature for Azo-COOH BZ (199 °C) shifted from 263 °C for conventional 3-phenyl-3,4-dihydro-2H-benzoxazine (Pa-type, without azo and carboxylic groups),⁵⁰ presumably because the azobenzene and carboxylic acid moieties acted as basic and acidic catalysts, respectively, that contributed to the lower polymerization

temperature. After thermal curing of pure Azo-COOH BZ at 180 °C, the intensity of the exotherm decreased upon increasing the curing temperature, only few enthalpy of curing after thermal curing at temperature between 180 and 240 °C. Figure 5 displays the FTIR spectra of Azo-COOH BZ at various stages during the curing process. The intensities of the characteristic absorption bands of the benzoxazine moiety—at 921 (C–O–C symmetric), 1232 (C–O–C asymmetric), and 1341 (CH₂ wagging) cm⁻¹—decreased upon increasing the curing temperature. After curing at 180 °C, these characteristic absorption bands of benzoxazine decreased, indicating that ring opening of the benzoxazine units had occurred. Nevertheless, some of these characteristic absorption bands—particularly at 921 (C–O–C symmetric) and 1232 (C–O–C asymmetric) cm⁻¹—remained after curing at 180 °C, implying that some of the benzoxazine rings had not opened. The result is consistent with the DSC analysis data, which revealed some enthalpy of curing (ca. 188 J g⁻¹) after thermal curing at 180 °C. Figure 6 displays TGA thermograms of Azo-COOH BZ before and after thermal curing under N₂ at 60, 110, 150, 180, and 210 °C. The thermal stability, the decomposition temperature (10 wt% loss), and the char yield all increased upon increasing the curing temperature, implying that increased crosslinking density (through hydrogen bonding) enhances the thermal stability of poly(Azo-COOH BZ). We observed that the degradation steps at 180 °C because of the decarboxylation process of carboxyl group.

Photoisomerization of Azobenzene Chromophore in Azo-COOH BZ

Figure 7 reveals evidence for the photoisomerization of the azobenzene chromophore in Azo-COOH BZ, through the change in the UV-Vis absorption spectrum of a solution of Azo-COOH BZ upon irradiation with UV light at 365 nm. The maximum

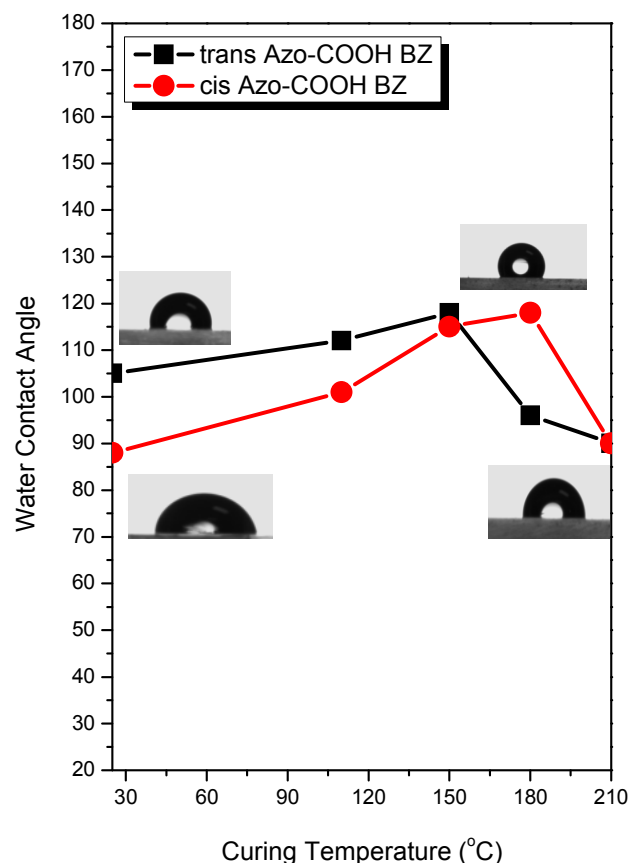


Figure 8. Water contact angles of Azo-COOH BZ in its trans and cis isomeric forms, recorded after each curing stage.

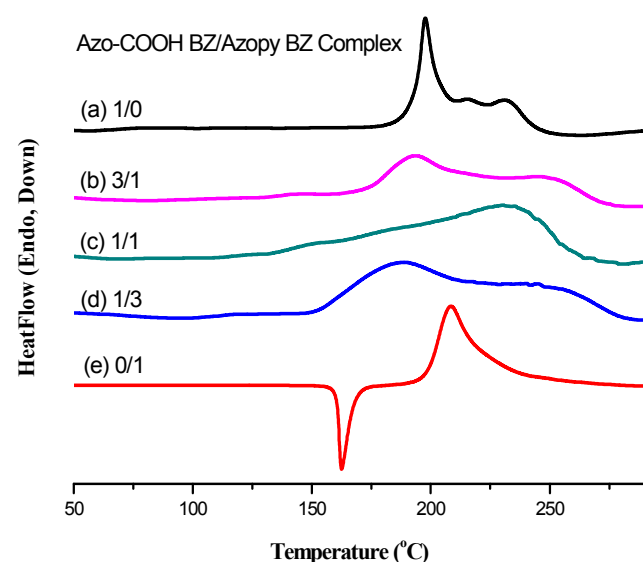


Figure 9. DSC thermograms of the Azo-COOH BZ/Azopy BZ supramolecular complex prior to thermal curing.

absorption at 360 nm is due to the $\pi-\pi^*$ transition of *trans*-azobenzene group. Upon irradiation with UV light, the intensity of the absorbance at 360 nm decreased gradually, ultimately reaching a stable value. These variations are consistent with *trans*-to-*cis* isomerization of the azobenzene unit in Azo-COOH

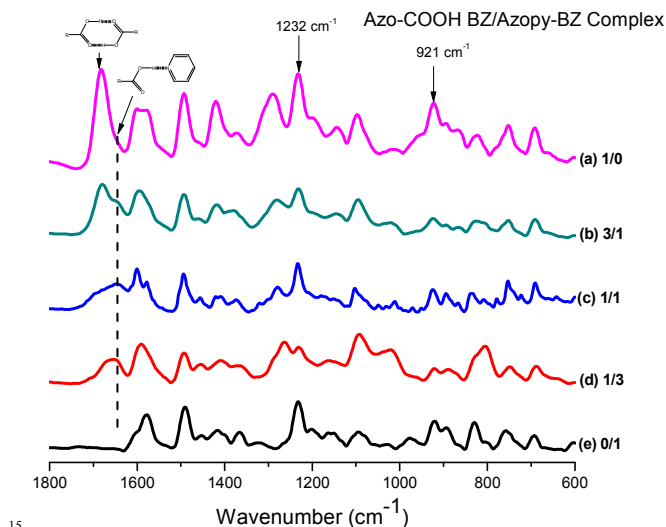


Figure 10. FTIR spectra of the Azo-COOH BZ/Azopy BZ supramolecular complex prior to thermal curing

BZ. The isomerization degree of mono-cyclic monomers at the photostationary state is calculated based on this equation:⁵¹

$$\text{Isomerization degree} = (A_0 - A_i) / A_0 \times 100\%$$

where A_0 is the absorbance at λ_{max} before the light irradiation and A_i is the absorbance at the same wavelength measured at the photostationary state. The isomerization degree of mono-cyclic monomers was 64 %. Figure 8 displays the contact angles of water on Azo-COOH BZ before and after its photoisomerization under a UV lamp at 365 nm, as well as after thermal curing at 110 and 150 °C for 3 h, at 180 °C for 2 h, and at 210 °C for 2 h.

We observed several interesting phenomena. First, the water contact angle, at room temperature, of the *trans* isomer of Azo-COOH BZ (105°) was larger than that of the *cis* isomer of Azo-COOH BZ (88°); this behavior is consistent with the *trans* isomer having a smaller dipole moment and lower surface free energy. Second, the surprisingly high water contact angle of the *trans* isomer (105°) was presumably due to strong intramolecular hydrogen bonding of the CO₂H group of Azo-COOH BZ. A similar result was found for a superhydrophobic surface (contact angle = 171°) consisting of fibers fabricated from amphiphilic poly(vinyl alcohol).⁵² Third, after thermal curing at 110, 150, 180, and 210 °C, the contact angles of the *trans* isomer were 112, 118, 96, and 90° respectively. Notably, after *trans*-to-*cis* photoisomerization of the Azo-COOH BZ samples that had been cured at 110, 150, 180, and 210 °C, the water contact angles became 101, 115, 118, and 90°, respectively. The water contact angles for the samples of the *trans* isomer increased after curing at 110 and 150 °C, presumably the result of a drying effect because our DSC analyses confirmed that the benzoxazine ring of Azo-COOH BZ would not open at a temperature at or below 150 °C. In contrast, the water contact angles decreased for the samples after curing at 180 and 210 °C because of ring opening of Azo-COOH BZ. This ring opening polymerization would result in the OH groups of the phenolic units forming intermolecular hydrogen bonds with the carboxylic acid groups, thereby decreasing the water contact angle. In addition, the *trans* and *cis* isomers of the Azo-COOH BZ sample displayed similar water contact angles after thermal curing at 210 °C, presumably because the *cis* isomer of Azo-COOH BZ transformed back to the *trans* isomer after thermal treatment at this elevated temperature. We emphasize that the water contact angles of these two isomers were complicated because they depended on the ratio of the photo-isomers of the azobenzene groups, the degree of thermal

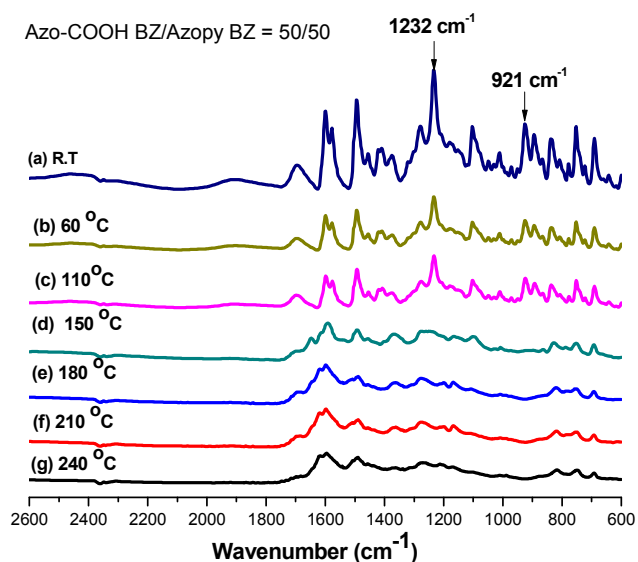


Figure 11. FTIR spectra of the Azo-COOH BZ/Azopy BZ = 50/50 complex, recorded after each heating stage.

curing, and the degree of intermolecular hydrogen bonding after thermal curing.

Supramolecular Azobenzene-Containing Benzoxazine Complexes, Stabilized Through Carboxylic Acid–Pyridine Hydrogen Bonds

Figure 9 presents the thermal curing behavior of Azo-COOH BZ/Azopy BZ supramolecular complexes. Pure Azo-COOH BZ and Azopy-BZ exhibited maximum curing temperatures of 199 and 208 °C, respectively. Interestingly, blending Azo-COOH BZ with Azopy-BZ at different molar ratios (1:3, 1:1, 3:1) resulted in two maximum curing temperatures for the complexes, each shifted to lower temperature. The first exothermic peak shifted to 150 °C from 199 °C, consistent with the high basicity of the pyridine ring facilitating nucleophilic attack on the benzoxazine ring; the second exothermic peak appeared at 190–255 °C for the completely ring-opened benzoxazine. Figure 10 displays FTIR spectra of Azo-COOH BZ/Azopy BZ supramolecular complexes at various molar ratios (1:3, 1:1, 3:1), prior to thermal curing. In all complexes, the FTIR spectra confirmed the formation of hydrogen bonds between the pyridyl moiety and the CO₂H group. Some of the characteristic peaks of pyridyl moieties are sensitive to the presence of hydrogen bonds; for example, the signals at 1590, 1050, 993, and 625 cm⁻¹ shifted to 1600, 1067, 1011, and 634 cm⁻¹, respectively, after pyridyl groups hydrogen bonded with the CO₂H groups of poly(ethylene-co-methacrylic acid).⁵³ In this present study, we observed that the signal of the pyridyl group shifted to 1646 cm⁻¹ from 1590 and 1684 cm⁻¹ after blending Azopy BZ with Azo-COOH BZ, consistent with strong intermolecular hydrogen bonding in their Azo-COOH BZ/Azopy BZ complexes.

Figure 11 presents FTIR spectra of the thermal polymerization products of the Azo-COOH BZ/Azopy BZ = 50/50 complex after thermal curing at various temperatures. The spectrum of pure Azo-COOH BZ features signals for the C–C stretching vibrations of its 1,2,4-trisubstituted benzene ring at 1490 and 921 cm⁻¹, as mentioned above. After thermal curing at 150, 180, 210, and 240 °C, these characteristic bands had disappeared. Interestingly, a curing temperature of 150 °C was sufficient to complete benzoxazine ring opening of this supramolecular complex, in contrast to the behavior (Figure 5) of pure Azo-COOH BZ. Thus, the supramolecular complex formed

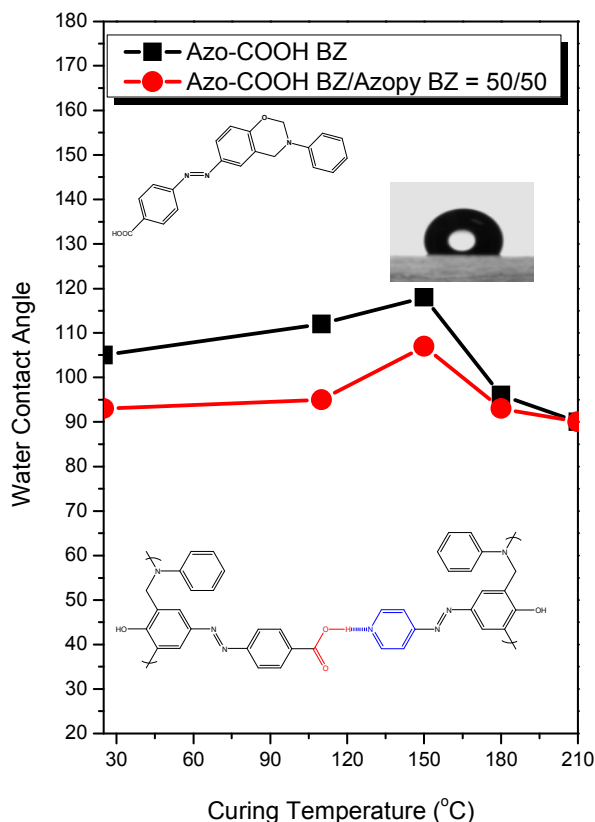


Figure 12. Water contact angles of the Azo-COOH BZ/Azopy BZ = 1:1 complex in its trans and cis isomeric forms, recorded after each curing stage.

from Azo-COOH BZ/Azopy BZ exhibited enhanced thermal curing because the high basicity of the pyridine ring facilitated nucleophilic attack on the benzoxazine ring.

Figure 12 displays the water contact angles of pure Azo-COOH BZ and the Azo-COOH BZ/Azopy BZ supramolecular complex. After interacting with Azopy BZ, the water contact angle of the trans isomer of the supramolecular complex was smaller than that of the trans isomer of pure Azo-COOH BZ after thermal curing at all temperatures, consistent with intermolecular hydrogen bonding between the CO₂H group of Azo-COOH BZ and the pyridyl group of Azopy BZ decreasing the hydrophobicity of the surfaces.

Conclusions

We have prepared a benzoxazine, Azo-COOH BZ, containing both azobenzene and CO₂H units. The polymerization temperature of Azo-COOH BZ is much lower than that of traditional benzoxazine monomers, because the CO₂H and azobenzene groups on the benzoxazine monomer serves as a catalyst for the polymerization. Furthermore, TGA revealed that the presence of the CO₂H group significantly improved the thermal stability and char yield of Azo-COOH BZ. When we performed polymerizations of Azo-COOH BZ after blending with various ratios of Azopy-BZ, DSC revealed that the curing temperature of Azo-COOH BZ decreased from 199 to 150 °C. Thus, blending Azopy BZ into Azo-COOH BZ facilitated thermal curing and enhanced the hydrophilicity of their surfaces as a result of intermolecular hydrogen bonding between their CO₂H and pyridyl groups.

Acknowledgment

This study was supported financially by the Ministry of Science and Technology, Republic of China, under contracts MOST103-2221-E-110-079-MY3 and MOST102-2221-E-110-008-MY3.

References

1. A. Chernykh, J. P. Liu, and H. Ishida, *Polymer* 2006, **47**, 7664-7669.
2. Y. Cheng, J. Yang, Y. Jin, D. Deng, and F. Xiao, *Macromolecules* 2012, **45**, 4085-4091.
3. C. F. Wang, S. W. Kuo, C. Lin, H. G. Chen, C. S. Liao, and P. R. Hung, *RSC Adv.* 2014, **4**, 36012-36016.
4. C. C. Yang, P. I. Wang, Y. C. Lin, and S. W. Kuo, *Polymer* 2014, **55**, 2044-2050.
5. H. Ishida, and D. J. Allen, *J. Polym. Sci.; Part B: Polym. Phys.* 1996, **34**, 1019-1030.
6. Y. Yagci, B. Kiskan, and N. N. Ghosh, *J. Polym. Sci.; Part A: Polym. Chem.* 2008, **47**, 5565-5576.
7. L. Qu, and Z. Xin, *Langmuir* 2011, **27**, 8365-8370.
8. B. Kiskan, A. L. Demirel, O. Kamer, and Y. Yagci, *J. Polym. Sci.; Part A: Polym. Chem.* 2008, **46**, 6780-6788.
9. C. I. Chou, and Y. L. Liu, *J. Polym. Sci.; Part A: Polym. Chem.* 2008, **46**, 6509-6517.
10. T. Agag, J. Liu, R. Graf, H. W. Spiess, and H. Ishida, *Macromolecules* 2012, **45**, 8991-8997.
11. W. H. Hu, K. W. Huang, and S. W. Kuo, *Polym. Chem.* 2012, **3**, 1546-1554.
12. H. Ishida, and H. Y. Low, *Macromolecules* 1997, **30**, 1099-1106.
13. W. C. Chu, J. G. Li, and S. W. Kuo, *RSC Adv.* 2013, **3**, 6485-6498.
14. W. H. Hu, K. W. Huang, C. W. Chiou, and S. W. Kuo, *Macromolecules* 2012, **45**, 9020-9028.
15. X. Ning, and H. Ishida, *J. Polym. Sci. Part B: Polym. Chem.* 1994, **32**, 921-927.
16. X. Ning, and H. Ishida, *J. Polym. Sci. Part A: Polym. Chem.* 1994, **32**, 1121-1129.
17. H. Y. Low, and H. Ishida, *J. Polym. Sci. Part B: Polym. Phys.* 1998, **36**, 1935-1946.
18. K. Hemvichian, A. Laobuthee, S. Chirachanchai, and H. Ishida, *Polym. Degrad. Stab.* 2002, **76**, 1-15.
19. K. W. Huang, and S. W. Kuo, *Macromol. Chem. Phys.* 2010, **211**, 2301-2311.
20. H. J. Kim, Z. Brunovska, and H. Ishida, *Polymer* 1999, **40**, 1815-1822.
21. Z. Brunovska, and H. Ishida, *J. Appl. Polym. Sci.* 1999, **73**, 2937-2949.
22. T. Agag, and T. Takeichi, *Macromolecules* 2001, **34**, 7257-7263.
23. L. Y. Liu, M. J. Yu, and I. C. Chou, *J. Polym. Sci.; Part A: Polym. Chem.* 2004, **42**, 5954-5963.
24. H. Ishida, and H. Y. Lee, *Polymer* 2001, **42**, 6971-6979.
25. Y. C. Su, S. W. Kuo, D. R. Yei, H. Xu, and F. C. Chang, *Polymer* 2003, **44**, 2187-2191.
26. B. Kiskan, Y. Yagci, and H. Ishida, *J. Polym. Sci.; Part A: Polym. Chem.* 2008, **46**, 414-420.
27. H. Y. Liu, W. Zhang, Y. Chen, and X. S. Zheng, *J. Appl. Polym. Sci.* 2006, **99**, 927-936.
28. J. Zhang, R. Xu, and D. Yu, *Eur. Polym. J.* 2007, **43**, 743-752.
29. B. Kiskan, D. Colak, E. A. Muftuoglu, I. Cianga, and Y. Yagci, *Macromol. Rapid Commun.* 2005, **26**, 819-824.
30. B. Kiskan, and Y. Yagci, *Polymer* 2005, **46**, 11690-11697.
31. Y. C. Wu, and S. W. Kuo, *Polymer* 2010, **51**, 3948-3955.
32. S. W. Kuo, and F. C. Chang, *Prog. Polym. Sci.* 2011, **36**, 1649-1696.
33. Y. Yagci, B. Kiskan, L. A. Demirel, and O. Kamer, *J. Polym. Sci. Part A: Polym. Chem.* 2008, **46**, 6780-6788.
34. D. K. Demir, A. M. Tasdelen, T. Uyar, W. A. Kawaguchi, A. Sudo, T. Endo, and Y. Yagci, *J. Polym. Sci. Part A: Polym. Chem.* 2011, **49**, 4213-4220.
35. J. Dunkers, and H. Ishida, *J. Polym. Sci. Part A: Polym. Chem.* 1999, **37**, 1913-1921.
36. R. Andreu, J. A. Reina, and J. C. Ronda, *J. Polym. Sci. Part A: Polym. Chem.* 2008, **46**, 6091-6101.
37. H. Zhang, and J. Ruehe, *Macromolecules* 2005, **38**, 4855-4860.
38. T. Tanaka, H. Ogino, and M. Iwamoto, *Langmuir* 2007, **23**, 11417-11420.
39. A. Natansohn, and P. Rochon, *Chem. Rev.* 2002, **102**, 4139-4176.
40. T. Asano, T. Yano, and T. Okada, *J. Am. Chem. Soc.* 2002, **124**, 8398-8405.
41. T. Asano, T. Yano, and T. Okada, *J. Org. Chem.* 1984, **49**, 4387-4391.
42. H. Lee, J. Pietrasik, and K. Matyjaszewski, *Macromolecules* 2006, **39**, 3914-3920.
43. C. J. Barrett, J. Mamiya, G. K. Yagar, and T. Ikeda, *Soft Matter* 2007, **3**, 1249-1261.
44. Y. Yu, and T. Ikeda, *Macromol. Chem. Phys.* 2005, **206**, 1705-1708.
45. C. F. Wang, Y. C. Su, S. W. Kuo, C. F. Huang, Y. C. Sheen, and F. C. Chang, *Angew. Chem. Int. Ed.* 2006, **45**, 2248-2251.
46. C. S. Liao, J. S. Wu, C. F. Wang, and F. C. Chang, *Macromol. Rapid Commun.* 2008, **29**, 52-56.
47. W. Jiang, G. Wang, Y. He, X. Wang, Y. An, Y. Song, and L. Jiang, *Chem. Commun.* 2005, 3550-3552.
48. M. G. Moahmed, W. C. Su, Y. C. Lin, C. F. Wang, J. K. Chen, K. U. Jeong, and S.W. Kuo, *RSC Adv.* 2014, **4**, 50373-50385.
49. H. D. Kim, and H. Ishida, *J. Phys. Chem. A* 2002, **106**, 3271-3280.
50. H. Ishida, *Handbook of Polybenzoxazine* 2011, **1**, 1-69.
51. Y. H. Deng, Y. B. Li, and X. G. Wang, *Macromolecules* 2006, **39**, 6590-6598.
52. L. Feng, Y. Song, J. Zhai, B. Liu, J. Xu, L. Jiang, D. Zhu, *Angew. Chem. Int. Ed.* 2003, **115**, 824-826.
53. J. Y. Lee, P. C. Painter, and M. M. Coleman, *Macromolecules* 1988, **21**, 954-960.

